Lens Component Deletion based on Differentiable Ray Tracing

Supplementary Material

6. PSF Comparison

In order to further demonstrate our PSF calculation results, we compared different PSF methods on a single lens. The ray sampling was 128×128, image-plane sampling was 63×63, and the image delta was $0.1\mu m$. All methods were performed without batch segmentation, and the results of a single PSF calculation are presented in the Fig. 9. The differences and similarities among different PSF calculation methods are summarized in Tab. 4.

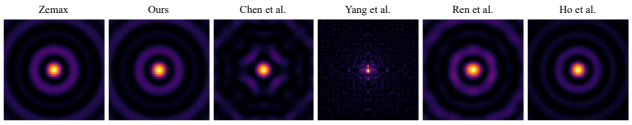

Figure 9. PSF estimation results of different methods (532.0 nm).

7. Lens Contribution

As illustrated in Fig. 10 and Fig. 11, for the initial Double Gauss and USP4488788, the most suitable components for deletion are the C4 and C4, respectively.

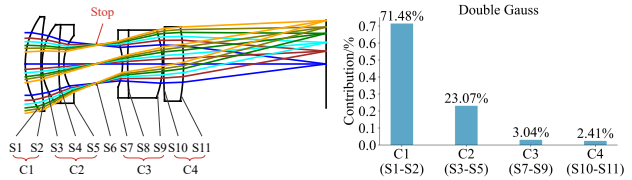

Figure 10. Contribution analysis of the Double Gauss: the most suitable component for deletion is the C4.

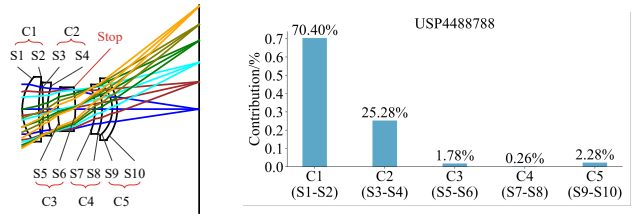

Figure 11. Contribution analysis of the USP4488788: the most suitable component for deletion is the C4.

8. Optical Loss Functions

The optical losses L_{opt} are primarily composed of the following loss functions:

Spot Loss: The spot diagram can demonstrate the imaging quality of a lens system directly. Using the spot diagram as the loss function is a simple and direct approach to correct transverse ray aberration. The spot loss function can be expressed as:

$$L_{spot} = \omega_{spot} \cdot \sum_{m=1}^{M} \sum_{n=1}^{N} \sum_{p=1}^{P} (x_{mnp} - \bar{x}_{mn})^2 + (y_{mnp} - \bar{y}_{mn})^2, \tag{19}$$

where M is the number of the wavelengths, N is the number of the fields of view, and P is the number of rays for each wavelength and field of view. The $\omega_{spot} = 200$ is the spot loss weight. The $\bar{x}_{mn}$ and $\bar{y}_{mn}$ can be expressed as:

$$\begin{cases} \bar{x}_{mn} = \dfrac{1}{P} \displaystyle\sum_{p=1}^{P} x_{mnp} \\ \bar{y}_{mn} = \dfrac{1}{P} \displaystyle\sum_{p=1}^{P} y_{mnp} \end{cases}. \tag{20}$$

Distortion Loss: The distortion quantifies the deviation of the chief ray from the ideal image point, which can be expressed as below:

$$dist_{mn} = \sqrt{\frac{(\hat{x}_{mn} - X_{mn})^2 + (\hat{y}_{mn} - Y_{mn})^2}{X_{mn}^2 + Y_{mn}^2}}, \tag{21}$$

where $(\hat{x}_{mn}, \hat{y}_{mn})$ denotes the coordinates of the chief ray for wavelength m and field of view n, while (X_{mn}, Y_{mn}) represents the coordinates of the ideal point. The distortion loss can be expressed as:

$$L_{dist} = \omega_{dist} \cdot \sum_{m=1}^{M} \sum_{n=1}^{N} \max(dist_{mn}^2 - T_{dist}^2, 0) \cdot (X_{mn}^2 + Y_{mn}^2), \tag{22}$$

where $\omega_{dist} = 1$ is the distortion loss weight, and T_{dist} is the target of the distortion.

Effective Focal Length Loss: The effective focal length is the basic specification that the system should meet. The effective focal length loss can be expressed as:

$$L_{efl} = \omega_{efl} \cdot (efl - T_{efl})^2, \tag{23}$$

where $\omega_{efl} = 1$ is the effective focal length loss weight, and T_{efl} is the target of the effective focal length.

Table 4. PSF estimation method comparison.

Methods	GPU Consumption for gradient computation	Differentiable	Diffraction	Phase Modulation Continuous / Discontinuous
Zemax[1]	-	✗	✓	✓/✗
Chen et al.[5]	-	✗	✓	✓/✗
Yang et al.[31]	Low	✓	✗	✓/✗
Ren et al.[17]	Low	✓	✓	✓/✗
Ho et al.[12]	High	✓	✓	✓/✓
Ours	Low	✓	✓	✓/✓

F-number Loss: The f-number is the basic specification that the system should meet. The f-number loss can be expressed as:

$$L_{fno} = \omega_{fno} \cdot (fno - T_{fno})^2, \tag{24}$$

where $\omega_{fno} = 1$ is the f-number loss weight, and T_{fno} is the target of the f-number.

Total Length Loss: The total length is the basic specification that the system should meet. The total length loss can be expressed as:

$$L_{ttl} = \omega_{ttl} \cdot \max(ttl - T_{ttl}, 0)^2, \tag{25}$$

where $\omega_{ttl} = 1$ is the total lengh loss weight, and T_{ttl} is the target of the total length.

Back Focal Length Loss: The back focal length is the basic specification that the system should meet. The back focal length loss can be expressed as:

$$L_{bfl} = \omega_{bfl} \cdot \max(T_{bfl} - bfl, 0)^2, \tag{26}$$

where $\omega_{bfl} = 1$ is the back focal length loss weight, and T_{bfl} is the target of the back focal length.

Minimum Glass Thickness Loss: The minimum glass thickness is the basic specification that the system should meet. The minimum glass thickness is related to the clear diameter of the glass element. The minimum glass thickness loss can be expressed as:

$$L_{gla\_min} = \omega_{gla\_min} \cdot \sum_{g=1}^{G} \max(R_{min} \cdot D_g - \delta_g, 0)^2, \tag{27}$$

where $\omega_{gla\_min} = 100$ is the minimum glass thickness loss weight, G is the number of glass elements, and $R_{min} = 0.1$ is the minimum ratio of thickness to diameter. D_g and δ_g are the clear diameter and the minimum thickness of the g-th glass element, respectively.

Maximum Glass Thickness Loss: The maximum glass thickness is the basic specification that the system should meet. The maximum glass thickness is related to the clear diameter of the glass element. The maximum glass thickness loss can be expressed as:

$$L_{gla\_max} = \omega_{gla\_max} \cdot \sum_{g=1}^{G} \max(\delta'_g - R_{max} \cdot D_g, 0)^2, \tag{28}$$

where $\omega_{gla\_max} = 1$ is the maximum glass thickness loss weight, G is the number of glass elements, and $R_{max} = 0.5$ is the maximum ratio of thickness to diameter. D_g and δ'_g are the clear diameter and the maximum thickness of the g-th glass element, respectively.

Minimum Air Thickness Loss: The minimum air thickness is the basic specification that the system should meet. The minimum air thickness loss can be expressed as:

$$L_{air\_min} = \omega_{air\_min} \cdot \sum_{a=1}^{A} \max(T_{air} - \delta_a, 0)^2, \tag{29}$$

where $\omega_{air\_min} = 100$ is the minimum air thickness loss weight, A is the number of air gaps, and $T_{air} = 0.05mm$ is the minimum air thickness boundary. δ_a is the minimum thickness of the a-th air gap.

Surface Slope Loss: The surface slope is the basic specification that the system should meet. The surface slope loss can be expressed as:

$$L_{slop} = \omega_{slop} \cdot \sum_{s=1}^{S} \sum_{p=1}^{P} \max(T_k - \cos(\overrightarrow{k_{sp}}, \overrightarrow{e_z}), 0) \tag{30}$$

where $\omega_{slop} = 1$ is the surface slope loss weight, $T_k = \cos 45^\circ$ is the slope boundary, and $\overrightarrow{e_z} = (0, 0, 1)$. S is the number of surfaces of the system and P is the number of rays. $\overrightarrow{k_{sp}}$ is the normal vector at the intersection point of the p-th ray with the s-th surface.

9. MTF Performance

Furthermore, we apply the spatial frequency response (SFR) to measure the modulation transfer function (MTF)

performance of the final results from various design methods across different fields of view. We provide the original imaging MTF performance of different designs, as illustrated in Fig. 12 and Fig. 13. The result restored by the joint design method demonstrates superior overall MTF performance.

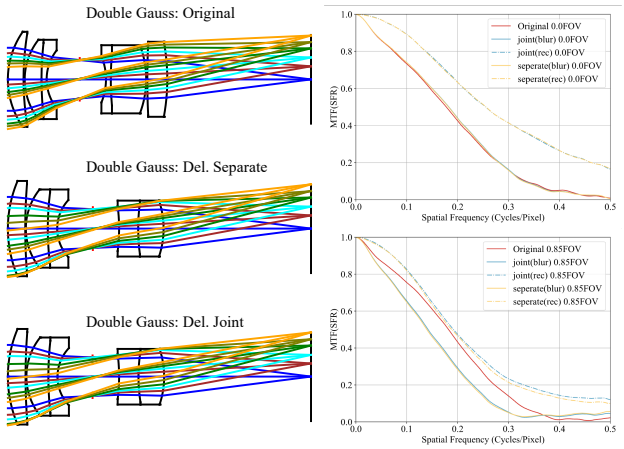

Figure 12. The MTF performances of different design methods based on Double Gauss (zoom in for details).

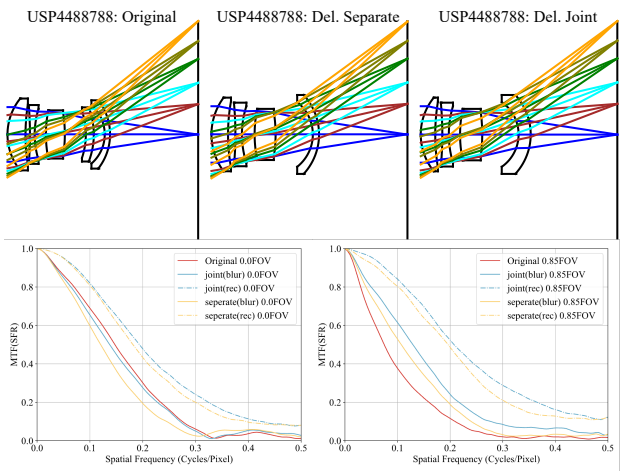

Figure 13. The MTF performances of different design methods based on USP4488788 (zoom in for details).

10. Performance on the Raise Dataset

We also validated our methodology on the Raise dataset [7], and the quantitative results are shown in Tab. 5. Based on the comprehensive analysis of previous results, the joint optimization of simplified lens systems demonstrates overall superior performance. It should be noted that the original lens systems used in our study were sourced directly from the lens patent database. Some of these original lenses may exhibit insufficient aberration correction, which could consequently lead to their imaging performance being inferior to that of the optimized simplified lens systems.

11. Additional Deletion Experiments

To future validate our proposed method, we provide additional lens deletion experiments: a large aperture telephoto lens USP4483597, and an objective lens ENLARGER (whose rear doublet is primarily designed to correct lateral chromatic aberration), as shown in Fig. 14. The experimental results are presented in Tab. 6.

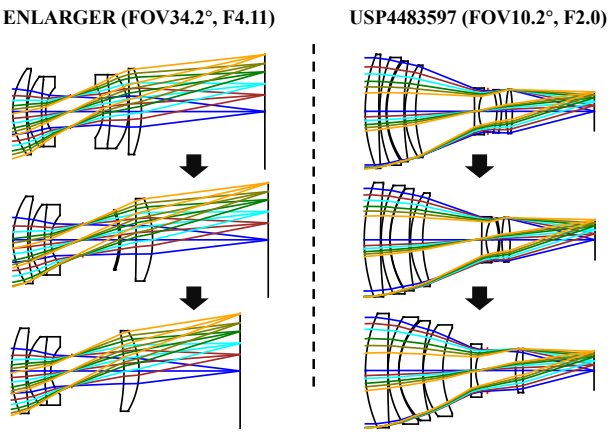

Figure 14. Component deletion process.

12. Tolerance Analysis

We consider three main tolerance types: decenter, tilt, and thickness deviations (including both glass and air thickness). Tolerances are $\pm 0.01mm$ for decenter, $\pm 1'$ for tilt, and $\pm 0.05mm$ for thickness. Before rendering each new image, we randomly sample a new set of tolerances, and the final Monte Carlo analysis results on the FiveK dataset are presented in Table 7. When considering tolerances, some simplified systems exhibit lower sensitivity (Double Gauss), while some demonstrate higher sensitivity (USP4483597, but the imaging gap remains minor compared to the original system). Overall, the effect of tolerances on the imaging quality of the simplified system (after recovery) is nearly equivalent to that on the original system.

13. Limitations

The contribution metric evaluates the extent of an element's contribution to the convergence of rays across all fields of view from both the perspective of power (P_i) and symmetry (A_i). This helps prevent severe ray divergence and deviations of first-order properties during the deletion process. Aberrations are not taken into account in the contribution

Table 5. Performance comparison of different design results on Raise dataset.

Lens	Methods	Imaging PSNR ↑ / SSIM ↑ / LPIPS ↓	Recovery PSNR ↑ / SSIM ↑ / LPIPS ↓	EFFL	F#	Avg Spot RMS
Double Gauss	Original	41.20/0.9822/0.0214	-/-/-	22.50mm	3.95	1.0μm
	Del. Seperate	39.17/0.9762/0.0234	39.50/0.9777/0.0173	22.50mm	3.95	1.2μm
	Del. Joint (Ours)	39.43/0.9771/0.0233	39.81/0.9789/0.0176	22.50mm	3.94	1.2μm
USP4488788	Original	36.00/0.9462/0.0847	-/-/-	6.83mm	3.20	3.5μm
	Del. Seperate	37.44/0.9632/0.0572	38.92/0.9699/0.0356	6.83mm	3.20	2.7μm
	Del. Joint (Ours)	37.86/0.9669/0.0459	39.54/0.9736/0.0279	6.83mm	3.20	2.5μm

Table 6. Additional comparison of different design results on FiveK dataset.

Lens	Methods	Imaging PSNR ↑ / SSIM ↑ / LPIPS ↓	Recovery PSNR ↑ / SSIM ↑ / LPIPS ↓	EFFL	F#	Avg Spot RMS
ENLARGER	Original	39.52/0.9737/0.0293	-/-/-	13.03mm	4.11	1.97 μm
	Del. Seperate	34.41/0.9372/0.0911	37.74/0.9534/0.0695	13.04mm	4.11	6.39 μm
	Del. Joint (Ours)	34.60/0.9389/0.0894	38.83/0.9628/0.0492	13.10mm	3.99	6.30 μm
USP4483597	Original	39.94/0.9738/0.0312	-/-/-	45.60mm	2.00	2.10 μm
	Del. Separate	39.26/0.9738/0.0326	40.77/0.9780/0.0206	45.60mm	2.00	2.31 μm
	Del. Joint (Ours)	39.81/0.9758/0.0309	41.37/0.9804/0.0179	45.60mm	1.99	2.29 μm

Table 7. Tolerance analysis on FiveK dataset.

Lens	Methods	Imaging (w/ Tol.) PSNR ↑ / SSIM ↑ / LPIPS ↓	Recovery (w/ Tol.) PSNR ↑ / SSIM ↑ / LPIPS ↓
Double Gauss	Original	38.05/0.9654/0.0419	-/-/-
	Ours	38.21/0.9673/0.0350	38.77/0.9700/0.0275
USP4488788	Original	32.74/0.9154/0.1212	-/-/-
	Ours	33.05/0.9232/0.1128	33.69/0.9323/0.1019
ENLARGER	Original	37.14/0.9608/0.0427	-/-/-
	Ours	34.27/0.9363/0.0934	37.72/0.9583/0.0549
USP4483597	Original	36.67/0.9565/0.0469	-/-/-
	Ours	35.83/0.9506/0.0608	36.41/0.9554/0.0510

metric, as we aim to offload some of the aberration correction burden onto the network. When the optical system is already extremely compact, or when the aberrations induced by component deletion become overly complex, the restoration results of the network may not be sufficiently good compared to the imaging results of the original lens.

14. Lens Parameters

Here, we provide the optical parameters of both the original lens system (Tab. 8, Tab. 9, Tab. 10, and Tab. 11) and the lens system with component deletion (Tab. 12, Tab. 13, Tab. 14, and Tab. 15).

Table 8. USP4488788 (original lens system)

Surface Type	Radius	Thickness	Material
Sphere 1	2.1161 (V)	0.6703 (V)	LAK10
Sphere 2	7.0094 (V)	0.1669 (V)	-
Sphere 3	-12.6401 (V)	0.1772 (V)	SF11
Sphere 4	3.3055 (V)	0.4159 (V)	-
Sphere 5	4.4945 (V)	0.6956 (V)	BASF2
Sphere 6 (stop)	-5.6930 (V)	0.7866 (V)	-
Sphere 7	-2.6822 (V)	0.2900 (V)	LF7
Sphere 8	-2.8432 (V)	0.4056 (V)	-
Sphere 9	-1.4324 (V)	0.1970 (V)	LF7
Sphere 10	-2.0432 (V)	3.2699 (V)	-

Table 9. Double Gauss (original lens system)

Surface Type	Radius	Thickness	Material
Sphere 1	7.5769 (V)	1.4113 (V)	BASF51
Sphere 2	25.7450 (V)	0.1125 (V)	-
Sphere 3	5.8269 (V)	1.5237 (V)	BAF3
Sphere 4	32.7893 (V)	0.4500 (V)	SF4
Sphere 5	4.1547 (V)	2.9829 (V)	-
Sphere 6 (stop)	inf	2.3780 (V)	-
Sphere 7	-5.6406 (V)	0.4500 (V)	SF10
Sphere 8	28.1611 (V)	3.1781 (V)	BASF51
Sphere 9	-8.8053 (V)	0.1125 (V)	-
Sphere 10	61.8828 (V)	1.8085 (V)	BASF51
Sphere 11	-19.1068 (V)	12.9773 (V)	-

Table 10. ENLARGER (original lens system)

Surface Type	Radius	Thickness	Material
Sphere 1	5.0531 (V)	0.9601 (V)	LAF2
Sphere 2	13.0419 (V)	0.0610 (V)	-
Sphere 3	3.9665 (V)	1.0008 (V)	PK2
Sphere 4	18.6370 (V)	0.2794 (V)	F4
Sphere 5	2.4968 (V)	1.7374 (V)	-
Sphere 6 (stop)	inf	2.2911 (V)	-
Sphere 7	-3.4204 (V)	0.4876 (V)	SF1
Sphere 8	-14.5461 (V)	1.3005 (V)	LAKN7
Sphere 9	-4.1529 (V)	0.0305 (V)	-
Sphere 10	-164.5280 (V)	0.8687 (V)	LAF2
Sphere 11	-8.6863 (V)	8.6527 (V)	-

Table 11. USP4483597 (original lens system)

Surface Type	Radius	Thickness	Material
Sphere 1	32.3096 (V)	2.8500 (V)	FK52
Sphere 2	189.4837 (V)	0.1900 (V)	-
Sphere 3	30.2100 (V)	1.3300 (V)	SF1
Sphere 4	19.2033 (V)	0.1900 (V)	-
Sphere 5	18.3392 (V)	3.6100 (V)	FK52
Sphere 6	64.9779 (V)	0.1900 (V)	-
Sphere 7	18.0023 (V)	2.2800 (V)	SSK4A
Sphere 8	30.5155 (V)	12.3500 (V)	-
Sphere 9	-781.8931 (V)	0.9500 (V)	SF8
Sphere 10	9.2789 (V)	1.9000 (V)	-
Sphere 11 (stop)	inf	1.9000 (V)	-
Sphere 12	-12.5609 (V)	0.9500 (V)	LAKN13
Sphere 13	-16.6653 (V)	0.9500 (V)	-
Sphere 14	23.8185 (V)	1.3300 (V)	LAH52
Sphere 15	-29.2165 (V)	17.2379 (V)	-

Table 12. USP4488788 (component deletion)

Surface Type	Radius	Thickness	Material
Sphere 1	2.1349 (V)	0.5184 (V)	LAK10
Sphere 2	6.8144 (V)	0.2566 (V)	-
Sphere 3	-12.5245 (V)	0.2288 (V)	SF11
Sphere 4	3.4228 (V)	0.4173 (V)	-
Sphere 5	4.3819 (V)	0.8018 (V)	BASF2
Sphere 6 (stop)	-5.8705 (V)	1.3072 (V)	-
Sphere 7	-1.4267 (V)	0.4422 (V)	LF7
Sphere 8	-2.1418 (V)	3.1195 (V)	-

Table 13. Double Gauss (component deletion)

Surface Type	Radius	Thickness	Material
Sphere 1	10.8729 (V)	1.5800 (V)	BASF51
Sphere 2	51.9478 (V)	0.0983 (V)	-
Sphere 3	5.6355 (V)	1.9827 (V)	BAF3
Sphere 4	28.0806 (V)	0.8341 (V)	SF4
Sphere 5	3.7567 (V)	3.1089 (V)	-
Sphere 6 (stop)	inf	2.4261 (V)	-
Sphere 7	-13.9612 (V)	1.7503 (V)	SF10
Sphere 8	16.0668 (V)	2.2986 (V)	BASF51
Sphere 9	-7.7993 (V)	13.2148 (V)	-

Table 14. ENLARGER (component deletion)

Surface Type	Radius	Thickness	Material
Standard 1	7.5645 (V)	1.0649 (V)	LAF2
Standard 2	21.3742 (V)	0.1715 (V)	-
Standard 3	3.6271 (V)	1.3665 (V)	PK2
Standard 4	18.6606 (V)	0.5119 (V)	F4
Standard 5	2.4394 (V)	1.3519 (V)	-
Standard 6 (stop)	inf	3.6924 (V)	-
Standard 7	-14.2594 (V)	1.0420 (V)	LAF2
Standard 8	-5.3218 (V)	7.0255 (V)	-

Table 15. USP4483597 (component deletion)

Surface Type	Radius	Thickness	Material
Standard 1	28.9692 (V)	4.6972 (V)	FK52
Standard 2	280.8153 (V)	0.0497 (V)	-
Standard 3	21.2826 (V)	2.2459 (V)	SF1
Standard 4	15.3878 (V)	0.0499 (V)	-
Standard 5	14.4271 (V)	5.0357 (V)	FK52
Standard 6	33.1912 (V)	0.0498 (V)	-
Standard 7	16.3866 (V)	4.1393 (V)	SSK4A
Standard 8	21.1760 (V)	6.0039 (V)	-
Standard 9	-368.8250 (V)	1.1115 (V)	SF8
Standard 10	9.5636 (V)	2.3914 (V)	-
Standard 11 (stop)	inf	5.8727 (V)	-
Standard 12	17.0364 (V)	1.5620 (V)	LAH52
Standard 13	4748.3221 (V)	14.9993 (V)	-